

## Unbounded quantum backflow in two dimensions

Maximilien Barbier <sup>1,2</sup>, Arseni Goussev <sup>3</sup>, and Shashi C. L. Srivastava <sup>4,5</sup>

<sup>1</sup>*Scottish Universities Physics Alliance, University of the West of Scotland, Paisley PA1 2BE, Scotland, United Kingdom*

<sup>2</sup>*Max-Planck-Institut für Physik komplexer Systeme, Nöthnitzer Strasse 38, D-01187 Dresden, Germany*

<sup>3</sup>*School of Mathematics and Physics, University of Portsmouth, Portsmouth PO1 3HF, United Kingdom*

<sup>4</sup>*Variable Energy Cyclotron Centre, 1/AF Bidhannagar, Kolkata 700064, India*

<sup>5</sup>*Homi Bhabha National Institute, Training School Complex, Anushaktinagar, Mumbai 400094, India*



(Received 11 November 2022; accepted 17 February 2023; published 7 March 2023)

Quantum backflow refers to the counterintuitive fact that the probability can flow in the direction opposite to the momentum of a quantum particle. This phenomenon has been seen to be small and fragile for one-dimensional systems, in which the maximal amount of backflow has been found to be bounded. Quantum backflow exhibits dramatically different features in two-dimensional systems that, in contrast to the one-dimensional case, allow for degenerate energy eigenstates. Here we investigate the case of a charged particle that is confined to move on a finite disk punctured at the center and that is pierced through the center, and normally to the disk, by a magnetic flux line. We demonstrate that quantum backflow can be unbounded (in a certain sense), which makes this system a promising physical platform regarding the yet-to-be-performed experimental observation of this fundamental quantum phenomenon.

DOI: [10.1103/PhysRevA.107.032204](https://doi.org/10.1103/PhysRevA.107.032204)

### I. INTRODUCTION

The principle of quantum superposition is at the heart of quantum theory. Some of its best known manifestations include the double-slit interference, Schrödinger's-cat states, and entanglement [1]. Quantum backflow (QB) is another, far less known manifestation of the superposition principle. The gist of the QB effect is the counterintuitive possibility for a quantum particle to move, in a certain sense, in the direction opposite to its momentum.

Originally, the QB problem was formulated for a free non-relativistic particle on a line [2]. The formulation proceeds as follows. A particle of mass  $\mu$  moves freely along the  $x$  axis, and its time-dependent wave function  $\psi(x, t)$  comprises only positive-momentum plane waves:

$$\psi(x, t) = \frac{1}{\sqrt{2\pi\hbar}} \int_0^\infty dp \tilde{\psi}(p) e^{ipx/\hbar - ip^2 t/2\hbar\mu}, \quad (1)$$

where  $\tilde{\psi}$  is the initial ( $t = 0$ ) momentum-space wave function of the particle. Equation (1) guarantees that the outcome of any momentum measurement performed on  $\psi$  is bound to be positive. The wave function is normalized to unity,

$$\int_{-\infty}^\infty dx |\psi(x)|^2 = \int_0^\infty dp |\tilde{\psi}(p)|^2 = 1.$$

Surprisingly, even though the momentum of the particle is (with certainty) positive, the corresponding probability current  $j(x, t)$ , given by

$$j(x, t) = \frac{\hbar}{\mu} \text{Im} \left( \psi^* \frac{\partial \psi}{\partial x} \right), \quad (2)$$

can be negative at some  $x$  and  $t$ : this fact is the essence of the QB effect. A natural way to quantify the strength of the effect is to consider the total probability transfer  $\Delta$  through a fixed spatial point, say,  $x = 0$ , over a fixed (but arbitrary) time interval, say,  $-T/2 < t < T/2$ :

$$\Delta = \int_{-T/2}^{T/2} dt j(0, t). \quad (3)$$

Numerical investigations have shown [2–4] that  $\Delta$  admits a lower bound, namely,

$$\inf_{\psi} \Delta = \Delta_{\text{line}} \simeq -0.0384517, \quad (4)$$

commonly referred to as the Bracken-Melloy bound. As of today, the exact value of  $\Delta_{\text{line}}$  remains unknown (lower and upper bounds for  $\Delta_{\text{line}}$  were obtained very recently [5]).

Equation (4) shows that the effect of QB is relatively weak for a particle on a line: only a tiny fraction, less than 4%, of the total probability can potentially be transported in the “wrong” direction. This limitation is exacerbated by the fact that quantum states exhibiting probability transfer close to  $\Delta_{\text{line}}$  are characterized by infinite spatial extent and infinite energy [6]. Due to such factors, a laboratory demonstration of QB remains an open challenge [7].

QB becomes more pronounced and more amenable to experimental observation when considered in a ring, rather than on a line [14]. More concretely, one considers a particle of

Published by the American Physical Society under the terms of the [Creative Commons Attribution 4.0 International](https://creativecommons.org/licenses/by/4.0/) license. Further distribution of this work must maintain attribution to the author(s) and the published article's title, journal citation, and DOI. Open access publication funded by the Max Planck Society.

mass  $\mu$  and electric charge  $q$  moving in a ring of radius  $R$ . The ring is pierced (normally to the plane of the ring) by a constant uniform magnetic field  $B$ . The (normalized) wave function  $\psi$  is here assumed to have a non-negative angular momentum: in this context, QB then manifests itself as the possibility for the probability current

$$j(\theta, t) = \frac{\hbar}{\mu R^2} \left[ \text{Im} \left( \psi^* \frac{\partial \psi}{\partial \theta} \right) - \frac{qR^2 B}{2\hbar c} |\psi|^2 \right] \quad (5)$$

to be negative, at some  $\theta$  and  $t$ , despite the particle's angular momentum being, with certainty, non-negative. The probability transfer  $\Delta$  through a fixed point on the ring, say,  $\theta = 0$ , over a time interval  $-T/2 < t < T/2$  is still given by Eq. (3) but now with the current (5). A numerical analysis has shown that [14]

$$\inf_{\psi} \Delta = \Delta_{\text{ring}} \simeq -0.116816 \quad (6)$$

and that the backflow-optimizing state is achieved for  $\hbar T/4\mu R^2 \simeq 1.163635$  and  $B = 0$ . Thus, QB in a ring can be over three times more pronounced than QB on a line. In addition to this, the backflow-optimizing state in a ring appears to have a finite energy (and, in view of the system's geometry, a finite spatial extent) [14].

Therefore, an important question is whether there are physical systems characterized by a probability transfer  $\Delta$  smaller than  $\Delta_{\text{ring}}$ . Most of the attention to date has been focused on one-dimensional systems, where the probability transfer  $\Delta$  has always been found to be bounded from below [2–4, 6, 14–20]. In this work, we rather consider a two-dimensional system.

Two-dimensional QB has been studied for a charged particle moving in a uniform vertical magnetic field in the infinite  $(x, y)$  plane in both the commutative [21] and noncommutative [22] cases. As was noted by Strange [21], a noteworthy feature of such a system compared to one-dimensional systems is that it allows for degenerate energy eigenstates, namely, Landau levels in [21]. In turn, superpositions of degenerate Landau levels yield time-independent local currents  $j$ . Furthermore, by carefully tuning the coefficients of such superpositions, negative azimuthal currents can be seen to arise from superpositions of positive-angular-momentum Landau levels, which is thus a manifestation of QB for such a system. Therefore, Landau levels allow for time-independent backflow currents. This feature is in stark contrast to the transient backflow currents obtained in one-dimensional systems and is potentially promising regarding the yet-to-be-performed experimental observation of the elusive effect of QB.

The Landau levels that arise for a charged particle in the infinite  $(x, y)$  plane [21] are infinitely degenerate. However, in an actual experiment the particle would be confined within a finite region of space, hence typically alleviating the degeneracy of the energy spectrum. Therefore, this naturally prompts the question, Can superpositions of degenerate energy eigenstates still allow for time-independent backflow currents in other, possibly finite, two-dimensional systems?

To answer that question, in the present work we consider a two-dimensional system where a charged particle is confined to move on a disk of finite radius  $R$  that is punctured at the center and pierced through the center and normally to the disk by a magnetic flux line. That is, we assume that the particle

is subjected to an Aharonov-Bohm potential. This particular system allows us to analytically compute the eigenenergies and corresponding eigenstates. We demonstrate the existence of superpositions of degenerate eigenstates that yield time-independent local backflow currents that, in addition, appear to be unbounded. Furthermore, since actual measurements typically correspond to some kind of space and time averages, we show the existence of time-independent spatially integrated backflow currents as well. Finally, we also show that our system allows for an unbounded dimensionless probability transfer  $\Delta$ , which is in stark contrast to the bounded probability transfers [such as (4) or (6)] obtained for one-dimensional systems. Our work hence extends the range of available physical platforms that can offer a practical advantage regarding the experimental observation of QB.

This paper is organized as follows. We first set up the problem in Sec. II and then formulate QB in Sec. III. We then discuss in Sec. IV how both the local current and the probability transfer are unbounded from below: this can be done by considering superpositions of two degenerate energy eigenstates. Concluding remarks are finally drawn in Sec. V.

## II. PUNCTURED DISK PIERCED BY A MAGNETIC FLUX

We consider a nonrelativistic structureless quantum particle of mass  $\mu$  and electric charge  $q$  confined on the punctured disk  $\mathcal{D}$ , with the center being the origin  $O$  and radius  $R > 0$ , defined by

$$\mathcal{D} \equiv \{\mathbf{r} \in \mathbb{R}^3 \mid 0 < r < R \text{ and } 0 \leq \theta < 2\pi\}. \quad (7)$$

The particle is subjected to the vector potential

$$\mathbf{A}(\mathbf{r}) = \frac{\eta}{r} \mathbf{e}_\theta, \quad (8)$$

where  $\eta$  is a fixed parameter whose dimension is (length  $\times$  energy)/(electric charge). The magnetic field corresponding to this vector potential,  $\mathbf{B}(\mathbf{r}) = \nabla \times \mathbf{A}(\mathbf{r})$ , vanishes for any  $\mathbf{r} \neq \mathbf{0}$ . Therefore, the particle on the punctured disk is subjected to zero magnetic field but to the nonzero vector potential (8). This scenario is thus reminiscent of the celebrated Aharonov-Bohm effect [23]. Such a situation can be realized by an ideal infinite solenoid, oriented along the  $z$  axis, that has a vanishing radius (see, e.g., [24]). The dynamical state  $|\Psi(t)\rangle$  of the particle at any time  $t$  is, in the position representation, described by a wave function  $\Psi(r, \theta, t)$  that obeys the time-dependent Schrödinger equation

$$i\hbar \frac{\partial}{\partial t} \Psi(r, \theta, t) = H \Psi(r, \theta, t), \quad (9)$$

where the Hamiltonian  $H$  is given by

$$\begin{aligned} H &= \frac{1}{2\mu} \left[ \mathbf{p} - \frac{q}{c} \mathbf{A}(\mathbf{r}) \right]^2 \\ &= -\frac{\hbar^2}{2\mu} \left[ \frac{\partial^2}{\partial r^2} + \frac{1}{r} \frac{\partial}{\partial r} + \frac{1}{r^2} \left( \frac{\partial}{\partial \theta} - i\beta \right)^2 \right] \end{aligned} \quad (10)$$

in terms of the dimensionless parameter  $\beta$  defined by

$$\beta \equiv \frac{q\eta}{\hbar c}, \quad (11)$$

with  $c$  denoting the speed of light (in vacuum).

Owing to the time independence and azimuthal symmetry of the Hamiltonian (10) and imposing periodic boundary conditions  $\psi(r, 0) = \psi(r, 2\pi)$  in the azimuthal direction as well as Dirichlet boundary conditions  $\lim_{r \rightarrow 0} \psi(r, \theta) = \psi(R, \theta) = 0$  in the radial direction, the normalized eigenstates that satisfy the time-independent Schrödinger equation are given by

$$\psi_{mn}(r, \theta) = \phi_{mn}(r) e^{im\theta}, \quad (12a)$$

with

$$\phi_{mn}(r) = \frac{1}{R\sqrt{\pi}} \frac{J_{|M|}(\gamma_{|M|n} \frac{r}{R})}{|J_{|M|+1}(\gamma_{|M|n})|}, \quad (12b)$$

where  $m$  is an arbitrary integer,  $n$  is a positive integer, and  $M$  is an arbitrary nonzero real number, defined by

$$M \equiv m - \beta. \quad (13)$$

The function  $J_{|M|}$  in (12b) is the Bessel function of the first kind of positive order  $|M|$  (hence irrespective of whether  $M$  itself is positive or negative), while  $\gamma_{|M|n}$  denotes the  $n$ th zero of  $J_{|M|}$ , that is,

$$J_{|M|}(\gamma_{|M|n}) = 0 \quad (14)$$

for any  $n \geq 1$ . The eigenstates (12) correspond to the eigenenergies  $E_{mn}$  given by

$$E_{mn} = \frac{\hbar^2}{2\mu R^2} \gamma_{|M|n}^2. \quad (15)$$

The complete set of eigenstates (12) is orthonormal,

$$\int_{\mathcal{D}} dS \psi_{mn}^*(r, \theta) \psi_{m'n'}(r, \theta) = \delta_{mm'} \delta_{nn'}, \quad (16)$$

where the asterisk (\*) denotes complex conjugation and  $\delta$  is the Kronecker delta. The dynamical state  $\Psi(r, \theta, t)$  of the particle at any time  $t$  can thus, in full generality, be expanded in terms of the eigenstates  $\psi_{mn}$  as

$$\Psi(r, \theta, t) = \sum_{m \neq \beta} \sum_{n \geq 1} c_{mn} \psi_{mn}(r, \theta) e^{-iE_{mn}t/\hbar}, \quad (17)$$

where the complex coefficients  $c_{mn}$  must satisfy the normalization condition

$$\sum_{m \neq \beta} \sum_{n \geq 1} |c_{mn}|^2 = 1 \quad (18)$$

but are otherwise arbitrary.

### III. FORMULATION OF THE QUANTUM BACKFLOW PROBLEM

The kinetic angular momentum  $L$  is defined by

$$\mathbf{L} \equiv \mathbf{r} \times \left[ \mathbf{p} - \frac{q}{c} \mathbf{A}(\mathbf{r}) \right] \quad (19)$$

and is purely vertical in the present case,

$$\mathbf{L} = L_z \mathbf{e}_z = -\hbar \left( i \frac{\partial}{\partial \theta} + \beta \right) \mathbf{e}_z. \quad (20)$$

It admits the energy eigenstates (12) as eigenstates, with  $L_z \psi_{mn} = M \hbar \psi_{mn}$ . The sign of  $M$  hence allows us to assign

a precise direction of motion (counterclockwise or clockwise) to the eigenstates  $\psi_{mn}$ .

The latter fact can also be viewed from the current. The probability current  $\mathbf{j}$  corresponding to  $\Psi$  is given by

$$\mathbf{j}(\mathbf{r}, t) \equiv \frac{1}{\mu} \text{Re} \left\{ \Psi^*(\mathbf{r}, t) \left[ \mathbf{p} - \frac{q}{c} \mathbf{A}(\mathbf{r}) \right] \Psi(\mathbf{r}, t) \right\}, \quad (21)$$

which in polar coordinates, and in view of Eq. (8), reads

$$\mathbf{j}(r, \theta, t) = j_r(r, \theta, t) \mathbf{e}_r + j_a(r, \theta, t) \mathbf{e}_\theta, \quad (22)$$

with

$$j_r(r, \theta, t) = -\frac{\hbar}{\mu} \text{Re} \left( i \Psi^* \frac{\partial \Psi}{\partial r} \right), \quad (23a)$$

$$j_a(r, \theta, t) = -\frac{\hbar}{\mu r} \left[ \text{Re} \left( i \Psi^* \frac{\partial \Psi}{\partial \theta} \right) + \beta |\Psi|^2 \right] \quad (23b)$$

being the radial and azimuthal components, respectively, of the current. It is then easy to check that evaluating the current for  $\Psi = \psi_{mn}$  yields

$$j_r(r, \theta, t)|_{\Psi=\psi_{mn}} = 0, \quad (24a)$$

$$j_a(r, \theta, t)|_{\Psi=\psi_{mn}} = \frac{M \hbar}{\mu r} |\phi_{mn}(r)|^2. \quad (24b)$$

This shows that the probability current  $\mathbf{j}$  for the eigenstates (12) is purely azimuthal and independent of the angle  $\theta$ . Furthermore, this ensures that  $\mathbf{j}|_{\Psi=\psi_{mn}}$  is oriented along  $+\mathbf{e}_\theta$  when  $M > 0$  and along  $-\mathbf{e}_\theta$  when  $M < 0$ .

Similar to the case of a charged particle in a one-dimensional ring [14] or in the infinite  $(x, y)$  plane [21,22], our formulation of QB is based on considering quantum states  $\Psi$  that contain only eigenstates  $\psi_{mn}$  with positive kinetic angular momentum; that is, we include only  $m > \beta$  in the expansion (17). Therefore, in the following we restrict ourselves to the class of states given by

$$\Psi(r, \theta, t) = \sum_{m > \beta} \sum_{n \geq 1} c_{mn} \psi_{mn}(r, \theta) e^{-iE_{mn}t/\hbar}, \quad (25)$$

with the normalization condition (18) now reading

$$\sum_{m > \beta} \sum_{n \geq 1} |c_{mn}|^2 = 1. \quad (26)$$

In view of (24), states of the form (25) hence correspond to superpositions of states  $\psi_{mn}$  that all individually exhibit a positive azimuthal current,  $j_a|_{\Psi=\psi_{mn}} > 0$ .

QB then occurs whenever the azimuthal component  $j_a$  of the probability current associated with the state (25) takes on negative values. In fact, there are three (closely related) quantities that can be used to quantify QB. Due to the rotational symmetry of the system, it is sufficient to introduce these quantities only for the points of the disk that lie on the ray  $\theta = 0$ .

First, the azimuthal probability current  $j_a$  quantifies the strength of QB locally in space and time. Thus, QB occurs at a spatial point  $(r, 0)$  and a time  $t$  whenever  $j_a(r, 0, t) < 0$ , and the smaller  $j_a$  is, the more pronounced QB is at this particular space-time point.

Second, the spatially integrated current

$$\mathcal{J}(r_1, r_2, t) = \int_{r_1}^{r_2} dr j_a(r, 0, t) \quad (27)$$

is the rate of probability transfer through the straight radial section of the disk connecting the points  $(r_1, 0)$  and  $(r_2, 0)$ , with  $0 < r_1 < r_2 \leq R$ , at a fixed time  $t$ . Clearly, the condition  $\mathcal{J}(r_1, r_2, t) < 0$  is stronger than the condition  $j_a(r, 0, t) < 0$  for some  $r_1 < r < r_2$ ; indeed, the former implies the latter, but not the other way around.

Third,

$$\Delta(r_1, r_2, T) = \int_{-T/2}^{T/2} dt \mathcal{J}(r_1, r_2, t) \quad (28)$$

is the total probability transfer through the straight section between  $(r_1, 0)$  and  $(r_2, 0)$  over the time interval  $-T/2 < t < T/2$ . The condition  $\Delta(r_1, r_2, T) < 0$  is stronger than  $\mathcal{J}(r_1, r_2, t) < 0$  for some  $-T/2 < t < T/2$ .

The dimensionless quantity  $\Delta$  defined by (28) is a two-dimensional analog of the probability transfer typically addressed in QB studies in one-dimensional settings [see Eq. (3)]. Remarkably, it behaves dramatically differently than its one-dimensional counterparts: while, in one dimension, the latter appear to be bounded from below [2–4,6,14–20], the two-dimensional probability transfer (28) is *unbounded from below*. This can be seen by considering a state that exhibits a time-independent backflow current, as we now discuss.

#### IV. TIME-INDEPENDENT BACKFLOW CURRENT

An important facet of QB in one-dimensional systems is the fact that the probability current  $j$  [given, e.g., by Eq. (2) in the line case and Eq. (5) in the ring case] can stay appreciably negative only for a finite time. The situation appears to be drastically different in two dimensions: indeed, as was noted by Strange for an electron in a constant magnetic field [21], the local current  $j_a$  can remain negative indefinitely.

To show that the latter fact remains true in our (finite) system it is sufficient to consider states  $\Psi$  composed of only two eigenstates,  $\psi_{mn}$  and  $\psi_{m'n'}$ , with, in accordance with (25),  $m > \beta$ ,  $m' > \beta$ ,  $n \geq 1$ ,  $n' \geq 1$ , and  $(m, n) \neq (m', n')$ . Furthermore, hereinafter we assume that  $\psi_{mn}$  and  $\psi_{m'n'}$  have the same energy, i.e.,

$$E_{mn} = E_{m'n'}. \quad (29)$$

In view of Eq. (15) [and remembering the definition (13)], this degeneracy condition is equivalent to the requirement that the  $n$ th zero of the Bessel function  $J_{m-\beta}$  coincides with the  $n'$ th zero of  $J_{m'-\beta}$  (which is not forbidden as long as  $m - \beta$  is irrational; see, e.g., [25]), i.e.,

$$\gamma_{m-\beta, n} = \gamma_{m'-\beta, n'}. \quad (30)$$

In view of (25) and (29), the state  $\Psi$  that we consider in the following hence reads

$$\Psi(r, \theta, t) = [c_{mn} \psi_{mn}(r, \theta) + c_{m'n'} \psi_{m'n'}(r, \theta)] e^{-iE_{mn}t/\hbar}, \quad (31)$$

subject to the normalization condition

$$|c_{mn}|^2 + |c_{m'n'}|^2 = 1. \quad (32)$$

The degeneracy conditions (29) and (30) are the crucial difference that distinguishes the two-dimensional system studied here from all the previous (one-dimensional) systems that have been considered to date regarding the maximal QB, for which degeneracy is *not* possible. We also note that the degeneracy condition (30) requires the presence of an external magnetic flux: indeed, if  $\beta = 0$ , the orders  $m - \beta$  and  $m' - \beta$  of the Bessel functions become integers, and distinct Bessel functions of integral orders are known to have no zeros in common (which is the so-called Bourget hypothesis; see, e.g., [25]).

#### A. Spatially local current $j_a$

Substituting Eqs. (31) and (12a) into Eq. (23b) immediately shows that the azimuthal local current  $j_a$  is time independent, and we have

$$j_a(r, 0) = \frac{\hbar}{\mu r} [ |c_{mn}|^2 M \phi_{mn}^2(r) + |c_{m'n'}|^2 M' \phi_{m'n'}^2(r) + \text{Re} \{ c_{mn}^* c_{m'n'} \} (M + M') \phi_{mn}(r) \phi_{m'n'}(r) ], \quad (33)$$

where, by definition,  $M = m - \beta$  [see Eq. (13)] and, similarly,  $M' = m' - \beta$ .

Our aim is now (i) to find the smallest possible value of the azimuthal current (33) and (ii) to demonstrate that this smallest value can be arbitrarily negative. The minimum of  $j_a$  over the space of all normalized expansion coefficients  $c_{mn}$  and  $c_{m'n'}$  is given by (see Appendix A for the derivation)

$$\min j_a = \frac{\hbar}{2\mu r} \{ M \phi_{mn}^2(r) + M' \phi_{m'n'}^2(r) - \sqrt{ [M \phi_{mn}^2(r) + M' \phi_{m'n'}^2(r)]^2 + (M - M')^2 \phi_{mn}^2(r) \phi_{m'n'}^2(r) } \} \quad (34a)$$

$$= \frac{\hbar}{2\mu r} \{ M \phi_{mn}^2(r) + M' \phi_{m'n'}^2(r) - \sqrt{ [M^2 \phi_{mn}^2(r) + M'^2 \phi_{m'n'}^2(r)] [\phi_{mn}^2(r) + \phi_{m'n'}^2(r)] } \}. \quad (34b)$$

First, it is clear from (34a) that  $\min j_a \leq 0$  for any  $r$ : the azimuthal current (33) can thus, indeed, be negative for states of the form (31). This is illustrated in Fig. 1 for a particular set of parameters, namely,  $(m, n) = (1, 3)$ ,  $(m', n') = (6, 1)$ , and  $\beta \approx 0.69$  [this value of  $\beta$  has been taken to satisfy the degeneracy condition (30) for the chosen values of  $m, n, m'$ , and  $n'$ ].

Furthermore, we now argue that  $\min j_a$  is unbounded from below (technical details can be found in Appendix B). To this end, let us consider some particular value(s) of  $r$  for which

$$\phi_{m'n'}^2(r) \sim \phi_{mn}^2(r) \sim O(1). \quad (35)$$

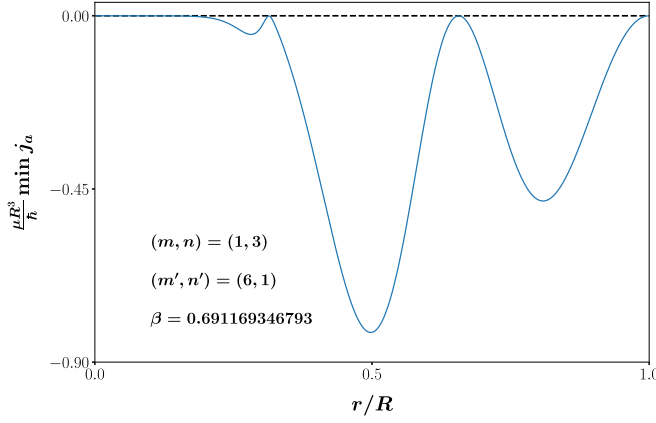


FIG. 1. (Dimensionless) minimum current  $(\mu R^3/\hbar) \min j_a$ , as given by (34), as a function of the (dimensionless) radial coordinate  $r/R$  for the set of parameters  $(m, n, m', n', \beta) = (1, 3, 6, 1, 0.691169346793)$ . The indicated value of  $\beta$  ensures the validity of the degeneracy condition (30).

Then, if we write  $M' = uM$ , we get upon combining (34b) with (35)

$$\min j_a \sim \frac{\hbar M \phi_{mn}^2(r)}{2\mu r} [1 + u - \sqrt{2(1+u^2)}]. \quad (36)$$

In the limit  $u \rightarrow \infty$  we then clearly see that

$$\min j_a \sim \frac{\hbar M \phi_{mn}^2(r)}{2\mu r} [1 + (1 - \sqrt{2})u] \xrightarrow{u \rightarrow \infty} -\infty. \quad (37)$$

This hence demonstrates that, by properly choosing the two degenerate eigenstates  $\phi_{mn}(r)$  and  $\phi_{m'n'}(r)$ , one can engineer an arbitrarily small current locally. (We note that the local backflow current has also been found to be unbounded in the one-dimensional case of a free particle on a line [2, 17].)

### B. Spatially integrated current $\mathcal{J}$

We now construct the spatially integrated current  $\mathcal{J}$ , as defined by (27), that is associated with the (time-independent) azimuthal current (33), and we get

$$\mathcal{J}(r_1, r_2) = \frac{\hbar}{\mu R^2} [|c_{mn}|^2 M S_{mmmn} + |c_{m'n'}|^2 M' S_{m'n'm'n'} + \text{Re} \{c_{mn}^* c_{m'n'}\} (M + M') S_{mmn'm'n'}], \quad (38)$$

where

$$S_{mmn'm'n'} = R^2 \int_{r_1}^{r_2} \frac{dr}{r} \phi_{mn}(r) \phi_{m'n'}(r). \quad (39)$$

Following the method outlined in Appendix A, we can here again find the smallest possible value  $\min \mathcal{J}$  of (38) over the space of all normalized expansion coefficients  $c_{mn}$  and  $c_{m'n'}$ , and we get

$$\min \mathcal{J} = \frac{\hbar}{2\mu R^2} (M S_{mmmn} + M' S_{m'n'm'n'} - \sqrt{[M S_{mmmn} - M' S_{m'n'm'n'}]^2 + (M + M')^2 S_{mmn'm'n'}^2}) \quad (40a)$$

$$= \frac{\hbar}{2\mu R^2} (M S_{mmmn} + M' S_{m'n'm'n'} - \sqrt{[M S_{mmmn} + M' S_{m'n'm'n'}]^2 + \rho}), \quad (40b)$$

where  $\rho$  is defined by

$$\rho = (M + M')^2 S_{mmn'm'n'}^2 - 4MM' S_{mmmn} S_{m'n'm'n'}. \quad (41)$$

Note that the quantity  $\rho$  given by (41) can take on both positive and negative values depending on the values of the parameters  $(m, n, m', n', \beta, r_1, r_2)$  (as we explicitly observe numerically). Therefore, as is clear from (40b),  $\min \mathcal{J}$  is negative only when  $\rho$  is positive: this is, for instance, the case for  $m = 1, n = 3, m' = 6, n' = 1, \beta \approx 0.69117, r_1 = 3R/10, r_2 = 7R/10$ , for which we indeed get  $\min \mathcal{J} < 0$ . However, we have not been able to find an argument that would allow us to conclude on either the boundedness or unboundedness of  $\min \mathcal{J}$ .

### C. Probability transfer $\Delta$

Finally, we now show that the probability transfer  $\Delta$  is unbounded from below. Since the integrated current (38) is, by construction, time independent, we hence readily get from the definition (28) of  $\Delta$  that

$$\Delta(r_1, r_2, T) = T \mathcal{J}(r_1, r_2). \quad (42)$$

We now choose the parameters  $(m, n, m', n', \beta, r_1, r_2)$  such that  $\mathcal{J}(r_1, r_2) < 0$  (which, as mentioned in Sec. IV B, can occur for  $m = 1, n = 3, m' = 6, n' = 1, \beta \approx 0.69117, r_1 = 3R/10, r_2 = 7R/10$ ). It is then immediately clear that

$$\lim_{T \rightarrow \infty} \Delta(r_1, r_2, T) = -\infty. \quad (43)$$

Therefore, it is clear from (42) and (43) that  $\Delta$  can be arbitrarily negative: as soon as  $\mathcal{J}(r_1, r_2) < 0$ , one then simply has to wait for a long enough time  $T$ . This is, in particular, a drastic difference from the (one-dimensional) ring case [14], where QB becomes weaker at large  $T$ .

## V. CONCLUSION AND OUTLOOK

We formulated and studied QB for a charged particle on a punctured disk. We saw that for such a finite two-dimensional system two quantifiers of QB, namely, the local azimuthal current (23b) and the dimensionless total probability transfer (28), are unbounded from below. This is, in particular, in stark contrast to the bounded probability transfers obtained to this date for one-dimensional systems. Similar to what Strange noticed for Landau levels in [21], this remarkable feature is seen to arise from the existence of superpositions of degenerate energy eigenstates [Eq. (31)] that give rise to time-independent backflow currents. Such time-independent backflow currents never arise in one-dimensional systems, where backflow currents are transient. Therefore, we believe that this makes two-dimensional systems in general, and the punctured disk studied in this work in particular, promising physical platforms that present a distinct practical advantage in view of the yet-to-be-performed experimental observation of the elusive phenomenon of QB.

While we have seen that degeneracy allows for an unbounded probability transfer  $\Delta$  as  $T \rightarrow \infty$  [Eq. (43)], it

would be interesting to study whether  $\Delta$  remains unbounded even for finite times  $T$ . Another possible follow-up question could be to investigate whether the unboundedness of  $\Delta$  actually requires degeneracy: in other words, is  $\Delta$  still unbounded for superpositions of eigenstates of different energies and thus for time-dependent currents?

Finally, we also point out that the punctured disk that we studied in this paper is an idealization. Indeed, in practice, the solenoid that creates the vector potential (8) necessarily has a finite radius  $\epsilon$ . Therefore, one would have to consider an annulus (rather than a disk) of finite inner radius  $\epsilon$  and outer radius  $R > \epsilon$ . It would thus be interesting to study how such a finite  $\epsilon$  would influence QB: for instance, what would be the impact of  $\epsilon$  on degeneracy?

**ACKNOWLEDGMENT**

M.B. is grateful to M. T. Eiles for valuable discussions.

**APPENDIX A: DERIVATION OF EQUATIONS (34a) AND (40a)**

Both the spatially local and spatially integrated currents, Eqs. (33) and (38), respectively, have the same dependence on the expansion coefficients  $c_{mn}$  and  $c_{m'n'}$ :

$$f = |c_{mn}|^2 A + |c_{m'n'}|^2 B + \text{Re} \{c_{mn}^* c_{m'n'}\} C, \quad (\text{A1})$$

where  $A, B,$  and  $C$  are constants. In order to find the minimum of  $f$  over the space of all normalized expansion coefficients, we parametrize the latter as

$$c_{mn} = \cos \frac{\varphi}{2}, \quad c_{m'n'} = e^{i\gamma} \sin \frac{\varphi}{2}, \quad (\text{A2})$$

with  $\varphi \in [0, \pi]$  and  $\gamma \in [0, 2\pi)$ . This yields

$$\begin{aligned} f &= A \cos^2 \frac{\varphi}{2} + B \sin^2 \frac{\varphi}{2} + C \cos \frac{\varphi}{2} \sin \frac{\varphi}{2} \cos \gamma \\ &= \frac{A+B}{2} + \frac{A-B}{2} \cos \varphi + \frac{C}{2} \sin \varphi \cos \gamma. \end{aligned}$$

Minimizing  $f$  with respect to  $\gamma$ , we find

$$\min_{\gamma} f = \frac{A+B}{2} + \frac{A-B}{2} \cos \varphi - \frac{|C|}{2} \sin \varphi.$$

In order to minimize the last expression with respect to  $\varphi$ , we perform the following transformation:

$$\begin{aligned} &(A-B) \cos \varphi - |C| \sin \varphi \\ &= \sqrt{(A-B)^2 + C^2} (\cos \varphi \cos \varphi_0 - \sin \varphi \sin \varphi_0) \\ &= \sqrt{(A-B)^2 + C^2} \cos(\varphi + \varphi_0), \end{aligned}$$

where  $\varphi_0 \in [0, \pi]$  is defined by

$$\cos \varphi_0 = \frac{A-B}{\sqrt{(A-B)^2 + C^2}}, \quad \sin \varphi_0 = \frac{|C|}{\sqrt{(A-B)^2 + C^2}}.$$

Then, the function

$$\min_{\gamma} f = \frac{1}{2} [A+B + \sqrt{(A-B)^2 + C^2} \cos(\varphi + \varphi_0)]$$

has a minimum at  $\varphi = \pi - \varphi_0$ , and

$$\min_{\varphi, \gamma} f = \frac{A+B - \sqrt{(A-B)^2 + C^2}}{2}. \quad (\text{A3})$$

Inserting adequate values of  $A, B,$  and  $C$  into (A3) and performing a few straightforward algebraic manipulations then readily yield expressions (34a) and (40a) of  $\min j_a$  and  $\min \mathcal{J}$ , respectively.

**APPENDIX B: UNBOUNDEDNESS OF  $\min j_a$**

In this Appendix we demonstrate the unboundedness of the spatially local current  $j_a$ , as described by Eqs. (35)–(37). We recall that we consider here couples of integers  $(m, n)$  and  $(m', n')$  such that  $m > \beta, m' > \beta, n \geq 1, n' \geq 1,$  and  $(m, n) \neq (m', n')$ : therefore, we have here

$$M \equiv m - \beta > 0, \quad M' \equiv m' - \beta > 0. \quad (\text{B1})$$

Furthermore, we assume the degeneracy condition (29), i.e.,

$$E_{mn} = E_{m'n'}, \quad (\text{B2})$$

that is, for the zeros  $\gamma_{m-\beta, n}$  and  $\gamma_{m'-\beta, n'}$  [Eq. (30)],

$$\gamma_{m-\beta, n} = \gamma_{m'-\beta, n'}. \quad (\text{B3})$$

For completeness, we also recall that we have [Eq. (12b)]

$$\phi_{mn}(r) = \frac{1}{R\sqrt{\pi}} \frac{J_M(\gamma_{Mn} \frac{r}{R})}{|J_{M+1}(\gamma_{Mn})|} \quad (\text{B4})$$

and

$$\phi_{m'n'}(r) = \frac{1}{R\sqrt{\pi}} \frac{J_{M'}(\gamma_{M'n'} \frac{r}{R})}{|J_{M'+1}(\gamma_{M'n'})|}, \quad (\text{B5})$$

as well as the minimal current [Eq. (34b)]

$$\begin{aligned} \min j_a &= \frac{\hbar}{2\mu r} \{M\phi_{mn}^2(r) + M'\phi_{m'n'}^2(r) \\ &\quad - \sqrt{[M^2\phi_{mn}^2(r) + M'^2\phi_{m'n'}^2(r)][\phi_{mn}^2(r) + \phi_{m'n'}^2(r)]}\}. \end{aligned} \quad (\text{B6})$$

We first introduce the parameter  $u$  defined through

$$M' \equiv uM, \quad (\text{B7})$$

as well as the function  $v(r)$  defined by

$$\phi_{m'n'}^2(r) \equiv v(r)\phi_{mn}^2(r). \quad (\text{B8})$$

We then rewrite (B6) in terms of these parameters  $u$  and  $v$ , and we get

$$\min j_a = \frac{\hbar M}{2\mu r} \phi_{mn}^2(r) \{1 + uv(r) - \sqrt{[1 + u^2v(r)][1 + v(r)]}\}. \quad (\text{B9})$$

We now derive a relevant upper bound for  $\min j_a$ . Since we know from the definitions (B1), (B7), and (B8) that [the case  $v(r) = 0$  is ruled out since in this case  $\min j_a = 0$ ]

$$u > 0, \quad v > 0, \quad (\text{B10})$$

we then clearly have

$$\begin{aligned} & \sqrt{[1 + u^2 v(r)][1 + v(r)]} \\ &= \sqrt{1 + v(r) + u^2 v(r) + u^2 v^2(r)} > \sqrt{u^2 v(r) + u^2 v^2(r)} \\ &= uv(r) \sqrt{1 + \frac{1}{v(r)}}, \end{aligned}$$

that is,

$$-\sqrt{[1 + u^2 v(r)][1 + v(r)]} < -uv(r) \sqrt{1 + \frac{1}{v(r)}},$$

and thus

$$\begin{aligned} & 1 + uv(r) - \sqrt{[1 + u^2 v(r)][1 + v(r)]} \\ & < 1 + uv(r) - uv(r) \sqrt{1 + \frac{1}{v(r)}}. \end{aligned} \quad (\text{B11})$$

Therefore, combining (B9) with (B11) yields the following inequality:

$$\min j_a < \frac{\hbar M}{2\mu r} \phi_{mn}^2(r) \left\{ 1 + uv(r) \left[ 1 - \sqrt{1 + \frac{1}{v(r)}} \right] \right\}, \quad (\text{B12})$$

which we emphasize is valid for any  $r$  where  $v(r) \neq 0$ .

Our aim is now to demonstrate that the right-hand side of inequality (B12) can achieve arbitrarily negative values at some well-chosen values of  $r$ . To this end, we first note that in view of (B10) we have

$$\sqrt{1 + \frac{1}{v(r)}} > 1,$$

so that

$$uv(r) \left[ 1 - \sqrt{1 + \frac{1}{v(r)}} \right] < 0. \quad (\text{B13})$$

Therefore, this *a priori* allows the right-hand side of (B12) to indeed be negative. A possible route could thus be to take the limit  $u \rightarrow \infty$ : this could make the right-hand side of (B12) decrease to  $-\infty$ , at least at some particular well-chosen values of  $r$ . However, demonstrating that this is, indeed, the case requires us to be careful about two things: (i) the value that  $\phi_{mn}^2(r)$  [which is a global factor on the right-hand side of (B12)] takes on at these particular values of  $r$  that we choose, which must be a *finite* (i.e., non-negligible) value for the right-hand side of (B12) to possibly go to  $-\infty$ , and (ii) the value of  $v(r)[1 - \sqrt{1 + 1/v(r)}]$  at these particular values of  $r$ , which must also be *finite* so as not to compensate the eventual growth of  $u$ .

Our strategy is thus as follows. First, we identify the values of  $r$  where  $\phi_{mn}^2(r)$  reaches a local maximum, hence ensuring in particular that  $\phi_{mn}^2(r)$  takes on finite values. This task can be tackled analytically by considering the regime  $u \gg 1$ , which allows us to rewrite  $\phi_{mn}^2(r)$  by means of asymptotic expansions of Bessel functions: this is discussed in Appendix B 1. We then argue in Appendix B 2 that  $v(r)[1 - \sqrt{1 + 1/v(r)}]$  remains finite at these particular values of  $r$ . We conclude in Appendix B 3.

TABLE I. Values of  $(m, n)$  and  $(m', n')$  yielding increasing values of  $u$ . The indicated values of  $\beta$  ensure the validity of both the degeneracy condition (30) and  $M' = uM$ . The first set of parameters that we consider here, namely,  $(m, n, m', n', \beta) = (1, 3, 6, 1, 0.691169346793)$ , corresponds to the set of parameters that we use in Fig. 1.

$m$	$n$	$m'$	$n'$	$\beta$	$u$
1	3	6	1	0.691169346793	17
1	9	23	1	0.8494862493541	147
1	28	80	1	0.957622423454	1865
1	102	308	1	0.973770549551	11705

### 1. Asymptotic expansion of $\phi_{mn}(r)$

From now on, we assume that the parameter  $u$  is very large,

$$u \gg 1. \quad (\text{B14})$$

Table I contains numerical evidence that it is, indeed, *a priori* possible to find values of the parameters  $(m, n, m', n', \beta)$  that (i) satisfy the degeneracy condition (B3) and (ii) yield values of  $u$  of increasing orders of magnitude, namely, from 10 to  $10^4$  here. Here we restricted our attention to  $m = n' = 1$ : this allowed us to perform a systematic search for all the corresponding parameters  $n, m'$ , and  $\beta$  that yield common zeros [i.e., such that (B3) is satisfied]. In this case, we observed that for any given  $n$  at most a unique couple of values  $(m', \beta)$  allows to satisfy the degeneracy condition. We have searched for all integers  $n$  between 3 and 164 and identified all the corresponding relevant values of  $m'$  (which take values between 6 and 501). Since such a numerical search is fundamentally bound to identify finite values, we hence assume that it remains possible to find arbitrarily large values of  $n$  and  $m'$  that will still satisfy the degeneracy condition (B3): this then ensures the validity of the regime (B14).

In view of the definition (B7) of  $u$ , our assumption (B14) is hence valid for

$$M \text{ fixed and } M' \gg 1. \quad (\text{B15})$$

Let us now quickly discuss the impact of our assumption (B14) on the degeneracy condition (B3). In view of (B15), it is clear that the zero  $\gamma_{M'n'}$  is thus a zero of the Bessel function  $J_{M'}$  of a large order. Therefore, since it is well known (see [25], pp. 485–486) that

$$\gamma_{M'n'} > M' \quad \forall n', \quad (\text{B16})$$

the degeneracy condition (B3) hence reads

$$\gamma_{M'n'} = \gamma_{Mn} > M' \gg 1. \quad (\text{B17})$$

The latter hence also requires, because  $M$  is fixed according to (B15), that

$$n \gg 1. \quad (\text{B18})$$

The fact that  $M$  is fixed and  $\gamma_{Mn} \gg 1$  now suggests that we rewrite  $\phi_{mn}(r)$  [as given by (B4)] by means of asymptotic expansions for Bessel functions of finite orders and large arguments. While this can be done without further assumption for  $J_{M+1}(\gamma_{Mn})$ , expanding  $J_M(\gamma_{Mn}r/R)$  requires us to assume that  $r/R$  is not negligible. Therefore, in the following we consider

only the portion of the disk away from the direct vicinity of the center of the disk; that is, we consider

$$r \in (R_1, R), \tag{B19}$$

where  $R_1$  is finite (for concreteness, we may, for instance, have in mind  $R_1 = R/2$ ). [The assumption (B19) is harmful for what we want to do here. Indeed, our numerical investigations strongly suggest anyway that  $\min j_a$  achieves its most negative values for finite values of  $r$  and for values of  $r$  that are closer and closer to  $R$  as we increase  $M'$ .]

We now use the well-known asymptotic expansion of a Bessel function of a fixed, finite order and very large argument [26,27], and we have

$$J_M\left(\gamma_{Mn}\frac{r}{R}\right) \sim \sqrt{\frac{2R}{\pi\gamma_{Mn}r}} \cos\left(\gamma_{Mn}\frac{r}{R} - \frac{M\pi}{2} - \frac{\pi}{4}\right) \tag{B20}$$

and

$$J_{M+1}(\gamma_{Mn}) \sim \sqrt{\frac{2}{\pi\gamma_{Mn}}} \cos\left[\gamma_{Mn} - \frac{(M+1)\pi}{2} - \frac{\pi}{4}\right]. \tag{B21}$$

Noting that

$$\cos\left[\gamma_{Mn} - \frac{(M+1)\pi}{2} - \frac{\pi}{4}\right] = \sin\left(\gamma_{Mn} - \frac{M\pi}{2} - \frac{\pi}{4}\right),$$

we hence get for (B21)

$$J_{M+1}(\gamma_{Mn}) \sim \sqrt{\frac{2}{\pi\gamma_{Mn}}} \sin\left(\gamma_{Mn} - \frac{M\pi}{2} - \frac{\pi}{4}\right). \tag{B22}$$

Substituting the asymptotic expansions (B20) and (B22) into (B4) hence yields the following asymptotic expansion of  $\phi_{mn}(r)$ :

$$\phi_{mn}(r) \sim \frac{1}{\sqrt{R\pi r}} \frac{\cos\left(\gamma_{Mn}\frac{r}{R} - \frac{M\pi}{2} - \frac{\pi}{4}\right)}{\left|\sin\left(\gamma_{Mn} - \frac{M\pi}{2} - \frac{\pi}{4}\right)\right|}. \tag{B23}$$

Now, since our aim is to identify some convenient values of  $r$  where  $\phi_{mn}(r)$  takes on finite values, we merely find the location of the extrema of  $\phi_{mn}$ . This is actually easily done by using the asymptotic expansion (B23): indeed, since  $\gamma_{Mn}r/R \gg 1$  here, the extrema of  $\phi_{mn}(r)$  can be approximated to be the extrema of the cosine function in the numerator in (B23) [this can be, e.g., seen from the function  $\cos(x)/\sqrt{x}$  and studying the equation that gives the stationary points of the latter function for large  $x$ ]. Therefore, let us denote by  $r_k$  these particular values of  $r$  where the numerator of  $\phi_{mn}(r)$  takes on its extremal values. These are determined by the condition

$$\gamma_{Mn}\frac{r_k}{R} - \frac{M\pi}{2} - \frac{\pi}{4} = k\pi, \quad k \in \mathbb{Z},$$

hence yielding

$$r_k = \frac{R}{\gamma_{Mn}} \left(k + \frac{M}{2} + \frac{1}{4}\right)\pi, \quad k \in \mathbb{Z}. \tag{B24}$$

Of course, the integer  $k$  in (B24) cannot actually be arbitrary since in view of (B19) we must have

$$R_1 < r_k = \frac{R}{\gamma_{Mn}} \left(k + \frac{M}{2} + \frac{1}{4}\right)\pi < R, \tag{B25}$$

that is,

$$\frac{\gamma_{Mn}}{\pi} \frac{R_1}{R} - \frac{M}{2} - \frac{1}{4} < k < \frac{\gamma_{Mn}}{\pi} - \frac{M}{2} - \frac{1}{4}. \tag{B26}$$

Therefore, for completeness we introduce the two integers  $k_{\min}$  and  $k_{\max}$ , defined by

$$k_{\min} \equiv \left\lfloor \frac{\gamma_{Mn}}{\pi} \frac{R_1}{R} - \frac{M}{2} - \frac{1}{4} \right\rfloor + 1 \tag{B27}$$

and

$$k_{\max} \equiv \left\lceil \frac{\gamma_{Mn}}{\pi} - \frac{M}{2} - \frac{1}{4} \right\rceil - 1, \tag{B28}$$

where  $\lfloor \cdot \rfloor$  and  $\lceil \cdot \rceil$  denote the floor and ceiling functions, respectively. The condition  $r_k \in (R_1, R)$  hence constrains the integer  $k$  in (B24) to take the values

$$k = k_{\min}, k_{\min} + 1, \dots, k_{\max} - 1, k_{\max}. \tag{B29}$$

In the following, we will focus our attention on the values of  $r_k$  that are close to the rim: that is, we will typically consider  $k = k_{\max}$ . The first advantage of doing this is that, compared to  $k_{\min}$ ,  $k_{\max}$  is independent of the (somehow artificial) parameter  $R_1$ . Another rationale for considering  $k = k_{\max}$  arises from the numerical observation that for values of  $k$  close to  $k_{\max}$  the particular positions  $r_k$  given by (B24) also turn out to accurately describe the locations of the local minima of the minimal current (B9) itself. This is, indeed, illustrated in Fig. 2 for the four sets of parameters  $(m, n, m', n', \beta)$  considered in Table I.

Since these particular positions  $r_k$  are the (approximate) locations of the extrema of  $\phi_{mn}(r)$ , they hence precisely correspond to the (approximate) locations of the *maxima* of  $\phi_{mn}^2(r)$ . In particular, we hence have at the position  $r = r_{k_{\max}}$

$$\phi_{mn}^2(r_{k_{\max}}) \sim \frac{1}{R\pi r_{k_{\max}}} \frac{1}{\sin^2\left(\gamma_{Mn} - \frac{M\pi}{2} - \frac{\pi}{4}\right)}, \tag{B30}$$

which is, indeed, *finite* [as the denominator in (B30) is bounded, it cannot make the right-hand side of (B30) arbitrarily small]. Of course, this particular position  $r_{k_{\max}}$  actually depends on  $n$ , which itself depends on  $M'$  because of the degeneracy condition (B17), and thus,  $r_{k_{\max}}$  also eventually depends on the parameter  $u$  that we will eventually send to infinity. But this is not an issue for what we want to do here: the only important thing for us is that we can actually find such a value of  $r$  for any set of parameters  $(m, n, m', n', \beta)$  that satisfies the degeneracy condition (B3).

## 2. The bracketed quantity in (B12)

Now that we have found the particular value  $r = r_{k_{\max}}$  at which the global factor  $\phi_{mn}^2(r)$  on the right-hand side of (B12) reaches a local maximum (and is thus non-negligible), we now set  $r = r_{k_{\max}}$  in (B12) to get

$$\begin{aligned} \min j_a|_{r=r_{k_{\max}}} &< \frac{\hbar M}{2\mu r_{k_{\max}}} \phi_{mn}^2(r_{k_{\max}}) \\ &\times \left\{ 1 + uv(r_{k_{\max}}) \left[ 1 - \sqrt{1 + \frac{1}{v(r_{k_{\max}})}} \right] \right\}. \end{aligned} \tag{B31}$$

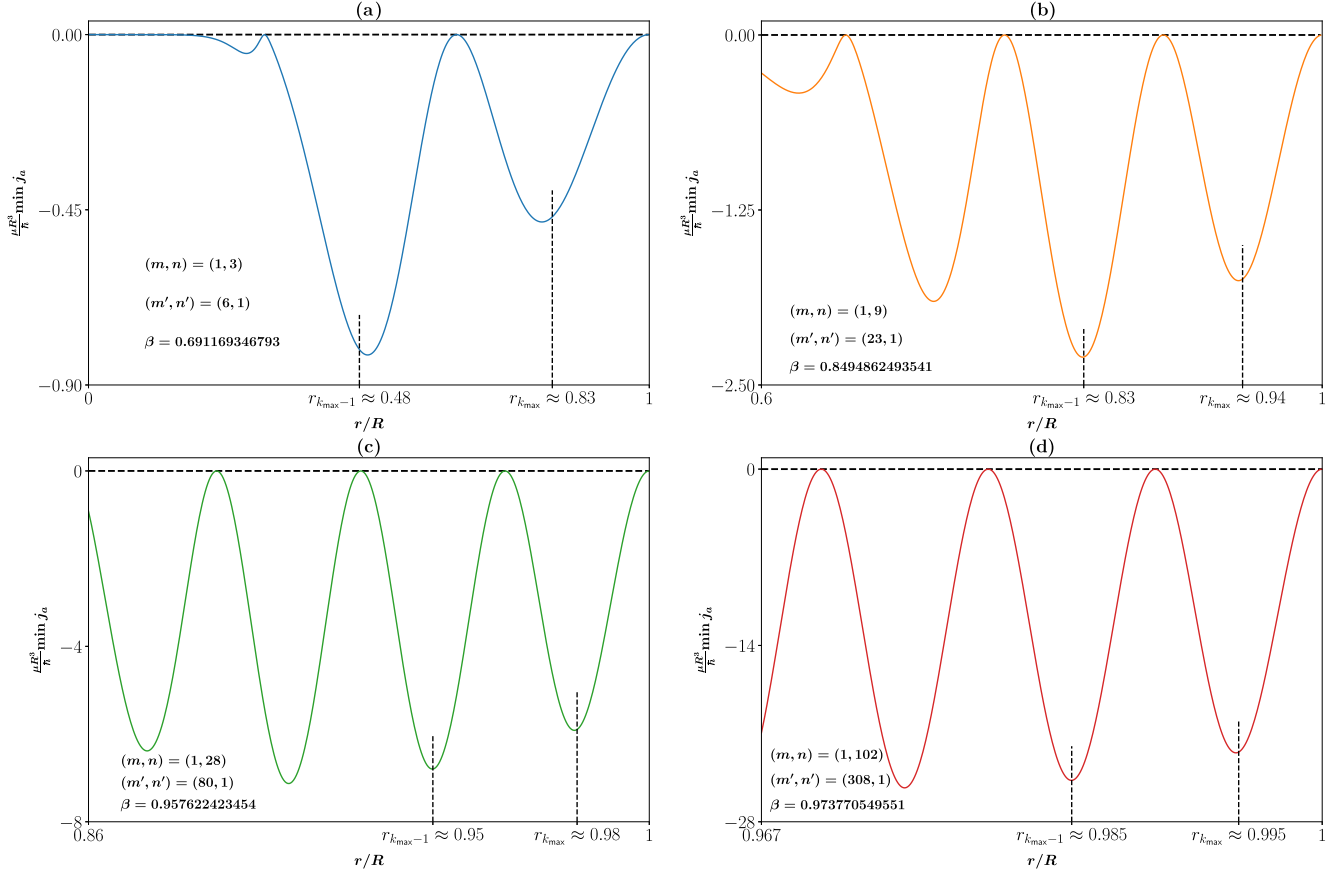


FIG. 2. (Dimensionless) minimum current  $(\mu R^3/h) \min j_a$ , as given by (B9), as a function of the (dimensionless) radial coordinate  $r/R$  for the four sets of parameters  $(m, n, m', n', \beta)$  considered in Table I. The corresponding values of the positions  $r_{k_{max}-1}$  and  $r_{k_{max}}$  are also indicated. (a) corresponds to the same set of parameters that we used in Fig. 1: we hence reproduced the latter here for completeness and for the purpose of comparing the resulting minimum current  $(\mu R^3/h) \min j_a$  obtained for other sets of parameters  $(m, n, m', n', \beta)$ .

We now argue that the term  $v(r_{k_{max}})[1 - \sqrt{1 + 1/v(r_{k_{max}})}]$  in (B31) cannot take negligible values as  $u \rightarrow \infty$ : this is, indeed, necessary for our argument since, otherwise, the actual value of the bracketed quantity on the right-hand side of (B31) cannot be guaranteed to be arbitrarily negative even in the limit  $u \rightarrow \infty$ .

To this end, we propose the following conjecture:

$$v(r_{k_{max}}) \gtrsim 1 \quad \text{however large } u \text{ is.} \quad (\text{B32})$$

Table II contains numerical evidence of the validity of this conjecture. Similar to what we did above to numerically investigate the validity of the regime (B14), here again we

TABLE II. Values of  $v(r_{k_{max}})$  for the four sets of parameters  $(m, n, m', n', \beta)$  considered in Table I.

$m$	$n$	$m'$	$n'$	$\beta$	$v(r_{k_{max}})$
1	3	6	1	0.691169346793	1.48137242921629
1	9	23	1	0.8494862493541	1.88363945185356
1	28	80	1	0.957622423454	2.15503028356504
1	102	308	1	0.973770549551	2.32355819487647

restrict our attention to  $m = n' = 1$ : we then also check the validity of our conjecture (B32) for all the valid sets of values of  $(n, m', \beta)$  for  $n$  between 3 and 164 (the corresponding valid values of  $m'$  are between 6 and 501). Furthermore, for these valid values of  $(m, n, m', n', \beta)$ , we observe that  $v(r_{k_{max}})$  actually seems to increase with  $n$  (and thus also with  $m'$ ): this hence makes our conjecture (B32) indeed reasonable.

Now, it is clear numerically that the function  $f(v) \equiv v[1 - \sqrt{1 + 1/v}]$  is monotonically decreasing, with the particular values  $f(0) = 0$ ,  $f(1) = 1 - \sqrt{2} \approx -0.41$ , and  $f(\infty) = -1/2$ . Therefore, we have, in view of our conjecture (B32), that  $f[v(r_{k_{max}})] \lesssim f(1) \approx -0.41$ ; that is, more explicitly,

$$v(r_{k_{max}}) \left[ 1 - \sqrt{1 + \frac{1}{v(r_{k_{max}})}} \right] \lesssim -0.41, \quad (\text{B33})$$

which hence indeed ensures that the term  $v(r_{k_{max}})[1 - \sqrt{1 + 1/v(r_{k_{max}})}]$  on the right-hand side of (B31) cannot take negligible values even in the limit  $u \rightarrow \infty$ , a limit that we can now safely take.

**3. Unboundedness of  $\min j_a$**

In view of (B33) we readily have (since  $u > 0$  by construction)

$$1 + uv(r_{k_{\max}}) \left[ 1 - \sqrt{1 + \frac{1}{v(r_{k_{\max}})}} \right] \lesssim 1 - 0.41u. \quad (\text{B34})$$

Taking the limit  $u \rightarrow \infty$  in (B34) hence yields

$$\begin{aligned} \lim_{u \rightarrow \infty} \left\{ 1 + uv(r_{k_{\max}}) \left[ 1 - \sqrt{1 + \frac{1}{v(r_{k_{\max}})}} \right] \right\} \\ \lesssim \lim_{u \rightarrow \infty} (1 - 0.41u) = -\infty, \end{aligned} \quad (\text{B35})$$

so that the left-hand side must tend to  $-\infty$ , i.e.,

$$\lim_{u \rightarrow \infty} \left\{ 1 + uv(r_{k_{\max}}) \left[ 1 - \sqrt{1 + \frac{1}{v(r_{k_{\max}})}} \right] \right\} = -\infty. \quad (\text{B36})$$

Therefore, we now take the limit  $u \rightarrow \infty$  in (B31); we get

$$\begin{aligned} \lim_{u \rightarrow \infty} \min j_a|_{r=r_{k_{\max}}} < \lim_{u \rightarrow \infty} \frac{\hbar M}{2\mu r_{k_{\max}}} \phi_{mn}^2(r_{k_{\max}}) \\ \times \left\{ 1 + uv(r_{k_{\max}}) \left[ 1 - \sqrt{1 + \frac{1}{v(r_{k_{\max}})}} \right] \right\}. \end{aligned} \quad (\text{B37})$$

That is, in view of (B36) and precisely because we constructed  $r_{k_{\max}}$  to ensure that the prefactor  $(\hbar M/2\mu r_{k_{\max}})\phi_{mn}^2(r_{k_{\max}})$  in (B37) remains finite,

$$\lim_{u \rightarrow \infty} \min j_a|_{r=r_{k_{\max}}} < -\infty, \quad (\text{B38})$$

finally,

$$\lim_{u \rightarrow \infty} \min j_a|_{r=r_{k_{\max}}} = -\infty. \quad (\text{B39})$$

This hence demonstrates that the spatially local current  $j_a$  is, indeed, unbounded from below.

---

[1] G. Aubrun, L. Lami, C. Palazuelos, and M. Plávala, Entanglement and Superposition Are Equivalent Concepts in Any Physical Theory, *Phys. Rev. Lett.* **128**, 160402 (2022).

[2] A. J. Bracken and G. F. Melloy, Probability backflow and a new dimensionless quantum number, *J. Phys. A* **27**, 2197 (1994).

[3] S. P. Eveson, C. J. Fewster, and R. Verch, Quantum inequalities in quantum mechanics, *Ann. Henri Poincaré* **6**, 1 (2005).

[4] M. Penz, G. Grübl, S. Kreidl, and P. Wagner, A new approach to quantum backflow, *J. Phys. A* **39**, 423 (2006).

[5] D. Trillo, T. P. Le, and M. Navascués, Quantum supremacy in mechanical tasks: Projectiles, rockets and quantum backflow, [arXiv:2209.00725](https://arxiv.org/abs/2209.00725).

[6] J. M. Yearsley, J. J. Halliwell, R. Hartshorn, and A. Whitby, Analytical examples, measurement models, and classical limit of quantum backflow, *Phys. Rev. A* **86**, 042116 (2012).

[7] It has been proposed that QB could be observed in Bose-Einstein condensates [8,9]. An alternative formulation of QB that could be more adapted to an experimental observation of this effect has been proposed [10,11]. Experimental realizations of an optical analog of QB have also been reported [12,13].

[8] M. Palmero, E. Torrontegui, J. G. Muga, and M. Modugno, Detecting quantum backflow by the density of a Bose-Einstein condensate, *Phys. Rev. A* **87**, 053618 (2013).

[9] S. Mardonov, M. Palmero, M. Modugno, E. Y. Sherman, and J. G. Muga, Interference of spin-orbit-coupled Bose-Einstein condensates, *Europhys. Lett.* **106**, 60004 (2014).

[10] M. Miller, W. C. Yuan, R. Dumke, and T. Paterek, Experiment-friendly formulation of quantum backflow, *Quantum* **5**, 379 (2021).

[11] M. Barbier and A. Goussev, On the experiment-friendly formulation of quantum backflow, *Quantum* **5**, 536 (2021).

[12] Y. Eliezer, T. Zacharias, and A. Bahabad, Observation of optical backflow, *Optica* **7**, 72 (2020).

[13] A. Daniel, B. Ghosh, B. Gorzkowski, and R. Lapkiewicz, Demonstrating backflow in classical two beams' interference, *New J. Phys.* **24**, 123011(2022).

[14] A. Goussev, Quantum backflow in a ring, *Phys. Rev. A* **103**, 022217 (2021).

[15] G. F. Melloy and A. J. Bracken, The velocity of probability transport in quantum mechanics, *Ann. Phys. (Berlin, Ger.)* **510**, 726 (1998).

[16] G. F. Melloy and A. J. Bracken, Probability backflow for a Dirac particle, *Found. Phys.* **28**, 505 (1998).

[17] H. Bostelmann, D. Cadamuro, and G. Lechner, Quantum backflow and scattering, *Phys. Rev. A* **96**, 012112 (2017).

[18] A. Goussev, Equivalence between quantum backflow and classically forbidden probability flow in a diffraction-in-time problem, *Phys. Rev. A* **99**, 043626 (2019).

[19] W. van Dijk and F. M. Toyama, Decay of a quasistable quantum system and quantum backflow, *Phys. Rev. A* **100**, 052101 (2019).

[20] J. Ashfaque, J. Lynch, and P. Strange, Relativistic quantum backflow, *Phys. Scr.* **94**, 125107 (2019).

[21] P. Strange, Large quantum probability backflow and the azimuthal angle-angular momentum uncertainty relation for an electron in a constant magnetic field, *Eur. J. Phys.* **33**, 1147 (2012).

[22] V. D. Paccioia, O. Panella, and P. Roy, Angular momentum quantum backflow in the noncommutative plane, *Phys. Rev. A* **102**, 062218 (2020).

[23] Y. Aharonov and D. Bohm, Significance of electromagnetic potentials in the quantum theory, *Phys. Rev.* **115**, 485 (1959).

[24] D. J. Griffiths, *Introduction to Electrodynamics*, 4th ed. (Pearson, Boston, 2013).

[25] G. N. Watson, *A Treatise on the Theory of Bessel Functions* (Cambridge University Press, Cambridge, 1966).

[26] I. S. Gradshteyn and I. M. Ryzhik, *Table of Integrals, Series, and Products*, 7th ed., edited by A. Jeffrey and D. Zwillinger (Elsevier/Academic, Amsterdam, 2007).

[27] M. Abramowitz and I. A. Stegun, *Handbook of Mathematical Functions with Formulas, Graphs, and Mathematical Tables*, edited by M. Abramowitz and I. A. Stegun, Applied Mathematics Series Vol. 55 (National Bureau of Standards, Washington, DC, 1964).